MSE307 Engineering Alloys 2014-15 L6: Microstructure Formation in Ti Alloys

D. Dye[a]

[a]*Rm G03b, Department of Materials, Imperial College London, London SW7 2AZ, UK. david.dye@imperial.ac.uk*

In this lecture we examine how microstructures are formed in $\alpha + \beta$ titanium alloys. On a 'typical' isomorphous phase diagram, Figure 1, we can make several observations. First, on the diagram, at zero β stabiliser content, there is still an $\alpha + \beta$ phase field, because in reality there will always be the presence of at least 500 ppmw oxygen (and potentially other α stabilisers), and often up to 2000 ppmw. Our prototypical titanium alloy, Ti-6Al-4V, which accounts for more Ti production than all the other alloys together (excluding commercially pure 'CP' Ti), retains some β phase to room temperature and so is termed an $\alpha + \beta$ alloy. There is a class of alloys we will meet later, near-α alloys, which retain only tiny amounts of α at room temperature. On the other hand there are alloys which should, in theory at least, have a Mo_{eq} high enough to retain an all β structure on quenching to room temperature, and these are termed 'metastable β' alloys. Beyond those, it may or may not be possible to produce fully stable β alloys - a subject of debate.

In any case, the key point for microstructure development in a 'typical' α+β alloy - by which people mean Ti64 - is that there is a two phase region at elevated temperature, below the β transus, where the material is fairly workable (soft and ductile). Conventional Ti processing consists of managing the fraction of α (temperature relative to the transus) in order to manipulate the microstructure. The transus for Ti-6Al-4V is at $1000 - 1050\,^{\circ}C$, depending on the O content.

In the β phase, grain growth is rapid up until a grain size of around $250 - 500\,\mu m$, and so whilst forging and recrystallisation can reduce the β grain size from cm to under a millimetre, it is very difficult to produce fine grained β grain structures. This is quite unlike steels, where with sufficient effort quite fine austenite grain sizes in the $1 - 20\,\mu m$ range are possible.

Then, on cooling from the β we first grow grain boundary films of α, Figure 2. The slower the cooling rate, the longer the time available to thicken these before the planar growth front decomposes and colony / Winmastatten / plate growth begins. As thick grain boundary α films are generally considered to be detrimental to toughness, fatigue initiation and fatigue crack growth, manufacturers try to avoid these. The α then grows in colonies from the grain boundary α, rejecting solute into the β and stabilising it against transformation. All the α plates in a colony will be of the same orientation, often inherited from the grain boundary α. Recall that there are 12 possible α orientations that can be inherited in each β grain. As the plates grow from all the grin boundaries (in 3D) to fill the grain, eventually the different colonies meet and so the prior β grain is filled with a relatively small number of

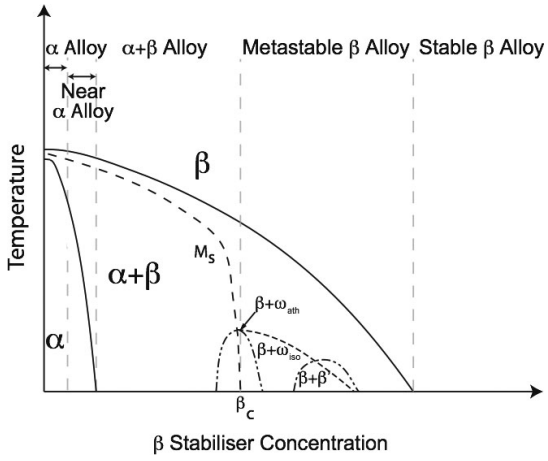

Figure 1: A schematic pseudo-binary phase diagram for titanium alloys. These are divided into α and near-α alloys, $\alpha + \beta$ alloys, and the heavily β-stabilised alloys.

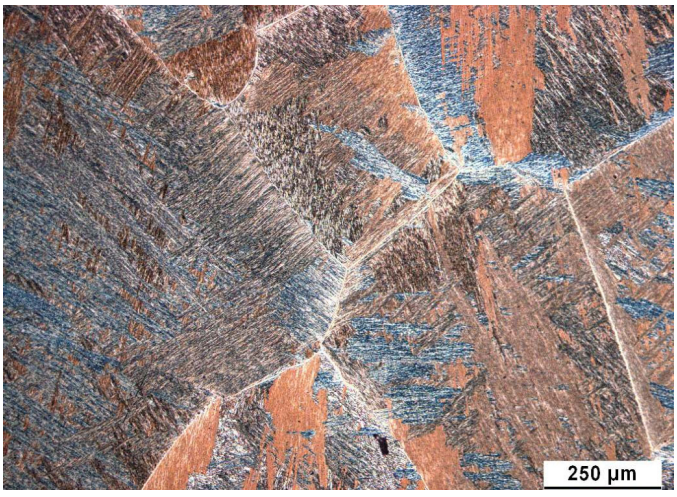

Figure 2: Colony microstructure formed in Ti-6246 by cooling from above the β transus. Figure from R Whittaker, PhD Thesis, U. Birmingham, 2011.

colonies.

Therefore nucleation generally only happens from the grain boundaries. This can be understood simply when one considers that β grain growth stagnates at the sorts of grain sizes that we see industrially - indicating that the dislocation density in the β is quite low (no driving force for growth) - and therefore there are few heterogenous nucleation sites. Of course, titanium being a reactive metal, there aren't oxide inclusions, as there will often be in steels, for example.

Ti-6Al-2Sn-4Zr-6Mo (Ti-6246) is an $\alpha - \beta$ alloy with a slightly greater β fraction than Ti-64, but with markedly slower precipitation kinetics. This is due to the high Mo content; Mo has a much slower diffusion rate in Ti than V (4d period rather than 3d; heavier elements tend to diffuse slower). In the micrograph we see Ti-6246 that has been reheated to near to the transus ($\sim 945\,^{\circ}\mathrm{C}$), slowly cooled and then allowed to cool rapidly in air. The larger laths are in a basket weave microstructure, rather than a colony structure; here the α forms with several habit planes at characteristic 60° angles. When the rapid cool began, a second generation of much finer α precipitated in between these laths.

Notice how fine the second generation - termed secondary α - can be. In the case in Figures 3 and 4, the finest α are $< 100\,\mathrm{nm}$ in width. These can give rise to a large amount of strengthening, presumably due to all of the $\alpha - \beta$ grain boundaries that must be traversed by

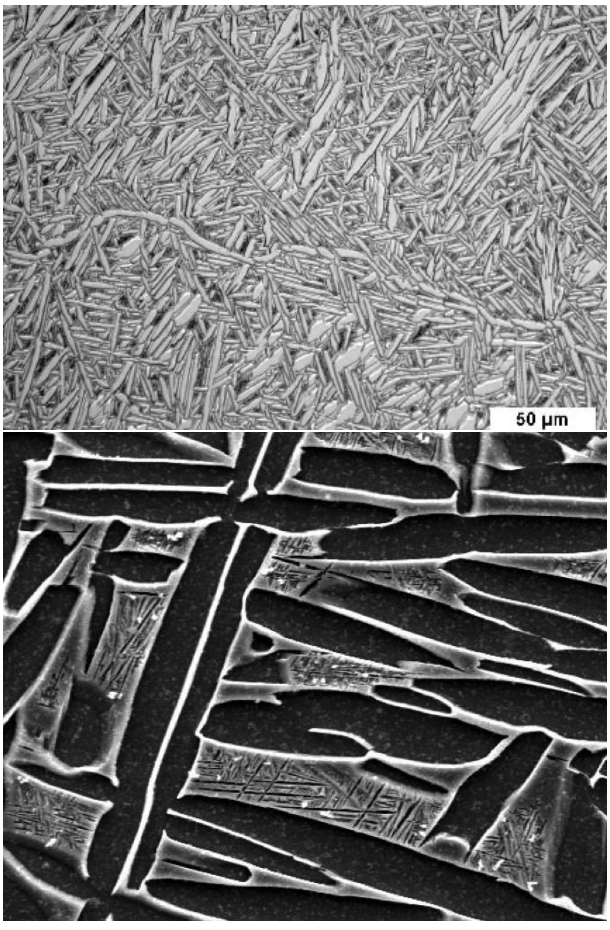

Figure 3: Basketweave microstructure formed in Ti-6246, with finer secondary α in between. Produced by cooling from near the transus to 820°C, then cooling rapidly in air. The α plates in the lower micrograph are around 1-2 µm in thickness. Figure from R Whittaker, PhD Thesis, U. Birmingham, 2011.

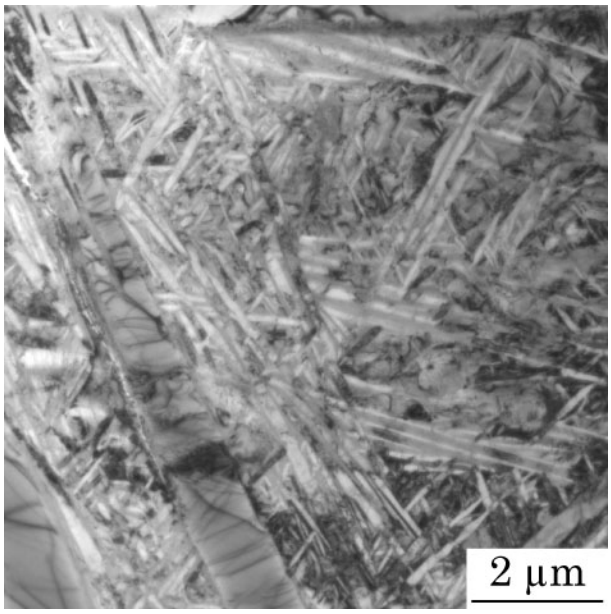

Figure 4: Secondary α laths (BF TEM) in between primary α in Ti-6246. Figure from TP Chapman, PhD Thesis, Imperial College, 2015.

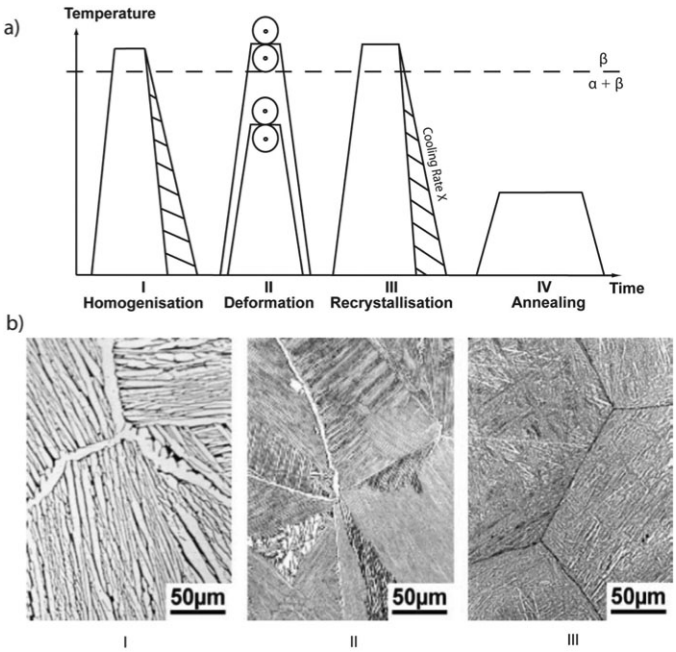

Figure 5: Generation of lamellar (β annealed) microstructures, e.g. in Ti-6Al-4V. The colony length is set by the cooling rate during the cooling from the last stage to go above the transus - I: $1\,\mathrm{K\,min^{-1}}$, II: $100\,\mathrm{K\,min^{-1}}$, III: $8000\,\mathrm{K\,min^{-1}}$. From Lutjering and Williams.

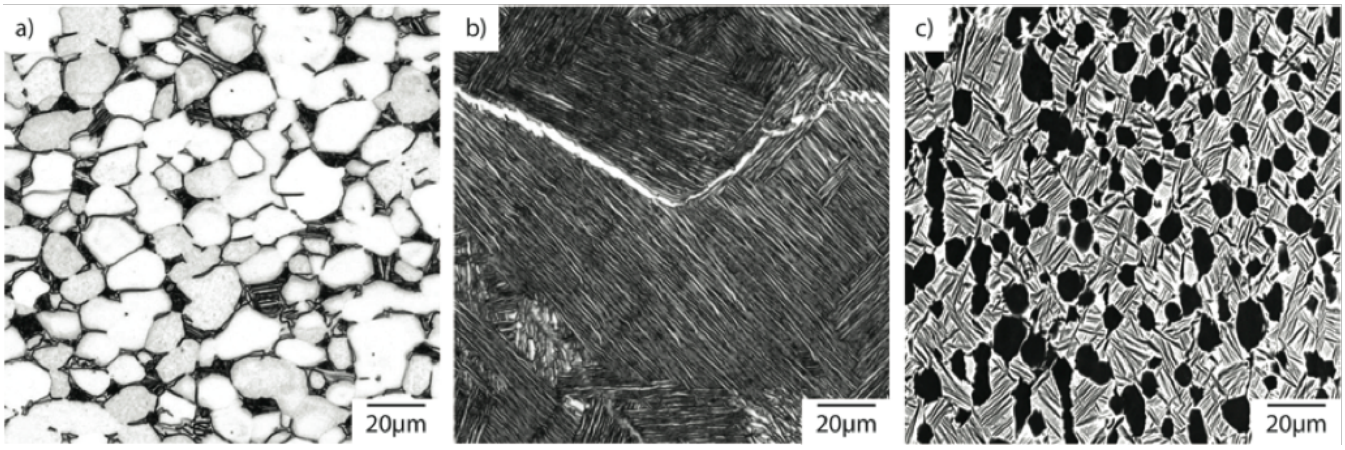

Figure 6: (a), (c) Bimodal microstructures, showing equiaxed primary α_p surrounded by laths of secondary α_s, in Ti-64 (a) and in Ti-6246 (c). In contrast, a lamellar α structure in Ti-64 is shown in (b),also showing grain boundary α (NG Jones and JL Warwick, Dye research group, 2011).

dislocations.

Therefore in classical Ti-64 processing, a lamellar microstructure is produced as shown schematically in Figure 5. The as-cast ingot is homogenised high in the β phase field where diffusion is rapid, followed by which it is deformed in either the $\alpha + \beta$ or β phase fields - although on grounds of ductility the first steps will usually be in the β. Then, the β is allowed to recrystallise in the β, and the α colony plate width is set by the cooling rate *at this stage*. Finally ,there may be annealing of the microstructure to get the compositions to uniform and equilibrium levels and to relieve and residual stresses from the cool. The recrystallisation and annealing steps might be omitted, but the key point is that the α plate width is set by the final cooling form the β that the part receives.

6.1. Breaking up the α plates

So as to mitigate the issues of strain localisation given by having large colonies of α that could deform as a single grain (potentially, on the single slip system that can traverse both α and β), then very often Ti microstructures are hot worked to produce fine equiaxed α grains. That is, the alloy is heated into the $\alpha + \beta$ region and deformed. This breaks up the α plates into equiaxed grains, as shown in Figure 6(a) and (c). In that Figure, (a)-(b) are light micrographs whereas (c) is a backscatter electron image (BSEI). As the β stabilisers are higher atomic number Z than the α stabilisers and therefore more effective at elastically scattering electrons, then typically in BSEI the β phase is brighter and so the contrast is reversed compared to light microscopy.

This process is shown schematically in Figure 7. The α plate width on cooling from the β after the β deformation and processing steps (I) sets the number density of the primary α. These plates are then deformed (II) in the $\alpha + \beta$ field and then recrystallised (III) in the $\alpha + \beta$ field. It is important to notice that the fraction of equiaxed α_p is set by the recrystallisation temperature (III) but their

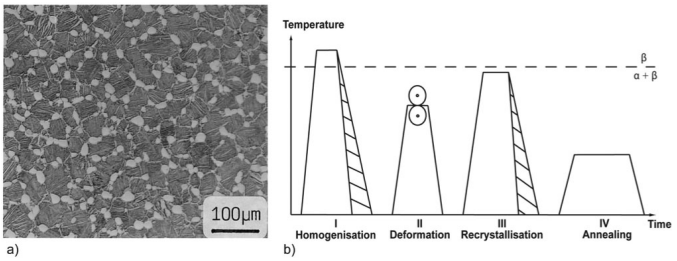

Figure 7: Generation of bimodal microstructures, e.g. in Ti-6Al-4V. The primary α_p plates are deformed in the $\alpha + \beta$ field and then recrystallised in the $\alpha + \beta$ field. From Lutjering and Williams.

number density is set by the cooling rate in (I). On cooling (III) any remaining α that is to be precipitated comes out of solution as laths, now called secondary α_s.

We can follow this process through rolling. Figure 8 shows the evolution of microstructure in Ti-6Al-4V that has been β heat treated and air cooled, then reheated back to 950 °C ($\sim$ 50% α fraction) and rolled. The rolling direction is denoted RD, normal direction of the sheet ND and the transverse direction TD. During rolling, the α plates are kinked and deformed until they begin to break up and dynamically recrystallise.

The α plates were then dissolved back to a fraction of around 50% and allowed to recrystallise, Figure 9. Regions of high curvature (dislocation content) are imagined to pinch off, enabling the α to globularise. After just 2hrs of what is termed recrystallisation annealing, the remnant of some of the plates are still - barely- visible, but at 4hrs they are largely not distinguishable by casual inspection.

In considering the secondary α_s, we return to consider the α/β orientation relationship. When we consider the lattice parameters of the two phases, we find that for each $\{110\}_\beta$, we can only fit one of the two <111> directions onto a $<11\bar{2}0>$, Figure 10. Since there are 6 distinct $\{110\}_\beta$, this means that there are 12 possible α orientation variants that can form from the β.

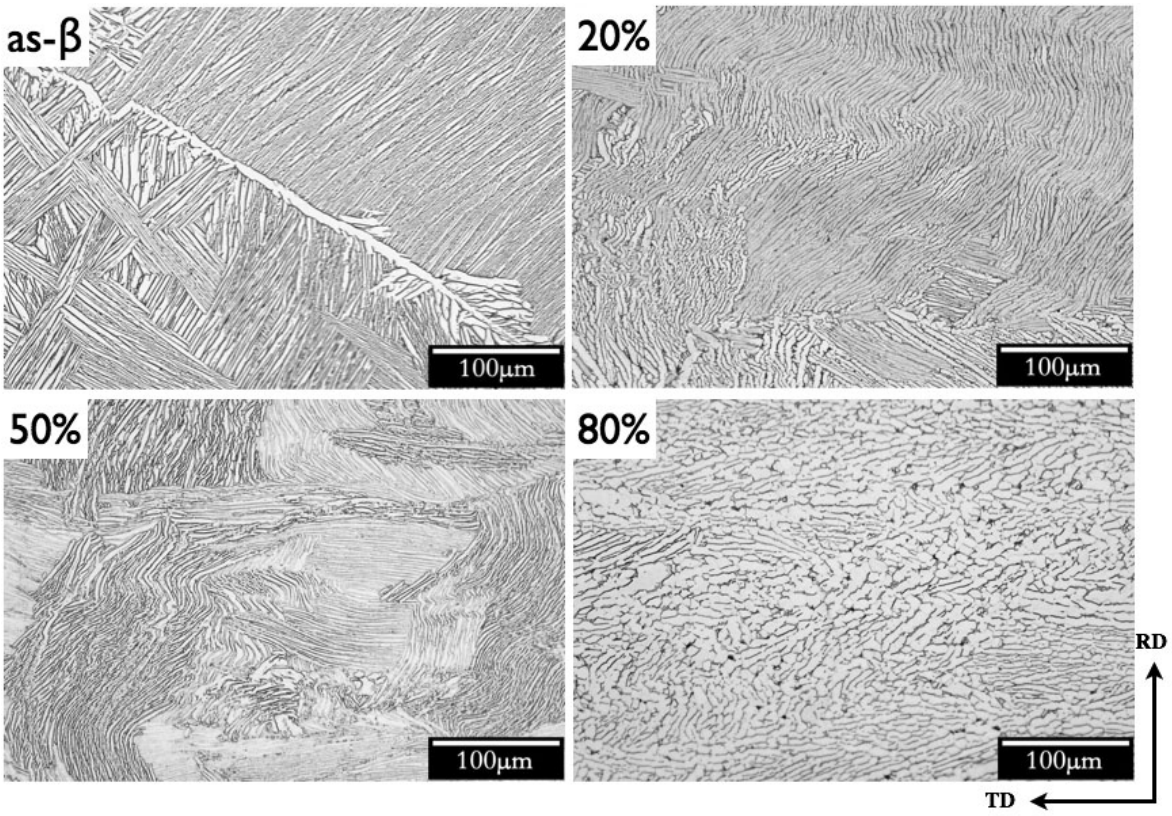

Figure 8: Ti-6Al-4V subjected to a β anneal at 1020 °C followed by air cooling. The plate was then cross rolled to nominal reductions of 20%, 50% and 80% at 950 °C. JL Warwick, Dye research group, 2013.

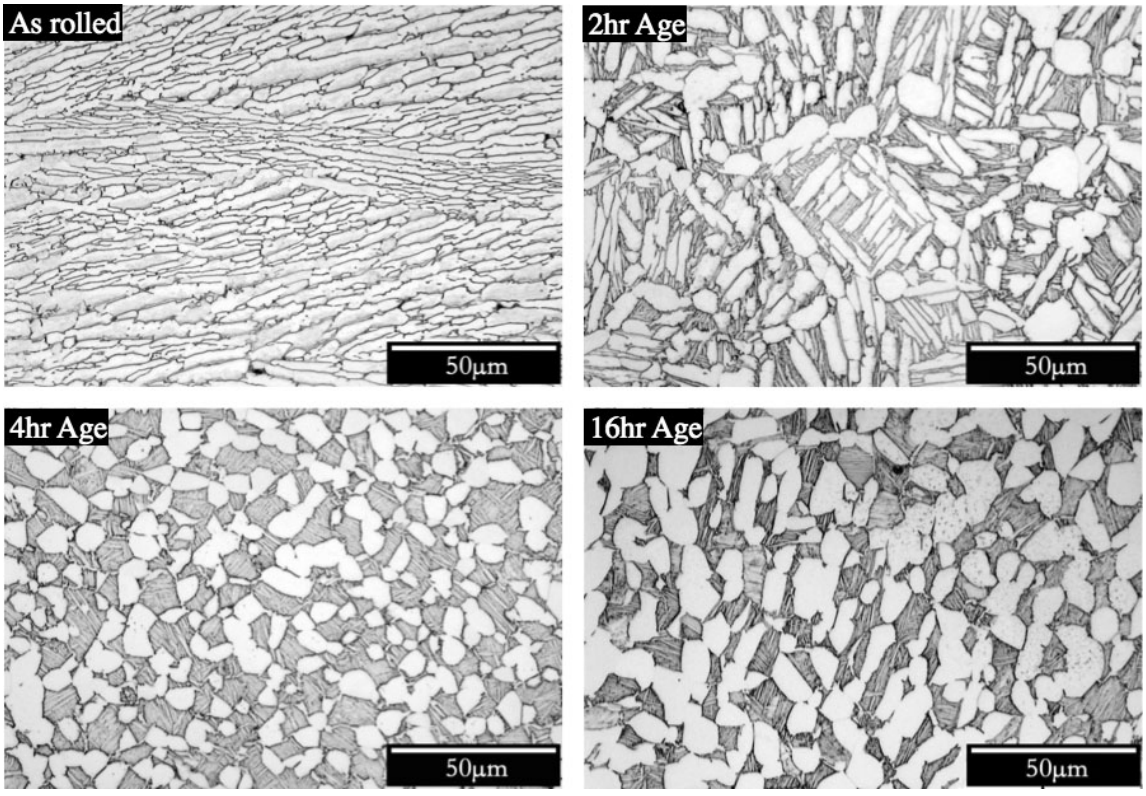

Figure 9: The 50% rolled material from Figure 8, then recrystallised at 950°C for 2, 4 and 16 hours. JL Warwick, Dye research group, 2013.

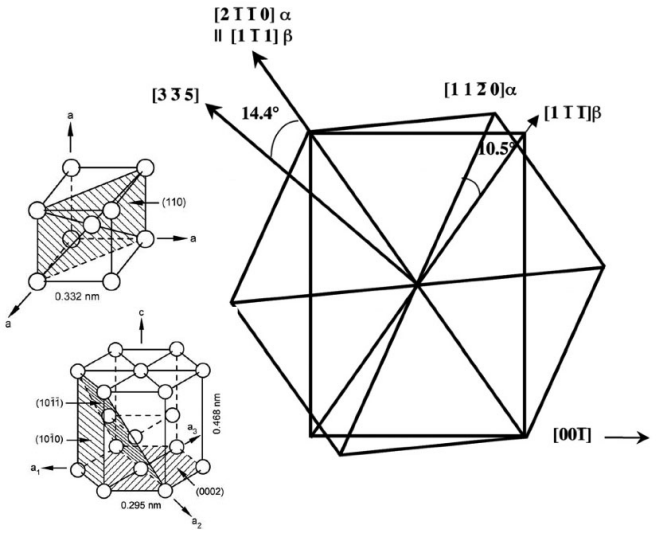

Figure 10: The α/β OR, {0002} ‖ {110}, $<11\bar{2}0>\|<111>$. Given the lattice parameters of the two phases, the $\{110\}_\beta$ plane doesn't fit perfectly on the α basal plane, so there is a 10.5° rotation on the non-fitted $<111>_\beta$. From Lutjering and Williams.

In the case of the α_s, these tend to form from the α_p in most circumstances. Therefore, whilst in bimodal processing we have apparently obtained a fine grained microstructure with $\sim 10\,\mu m$ α_p surrounded by even finder α_s plates, we may not have actually achieved very much variety of orientations. The α_p inherited their orientations form the parent colony lath α - there wasn't true recrystallisation, just globularisation. And so the α_p over quite large regions are found to be of similar orientation, as are their child secondary α.

This is depicted in Figure 11. These show the orientations in a region of the 4h annealed sample from Figure 9. Here, the colour denotes the cystallographic orientation of the normal to the sample (RD) in this case. The pole figures at the right plot the variation in the orientations measured. So, and (0002) pole figure shows the frequency variation in the distribution of (0002) plane normals with respect to the specimen direction. These are equal-area stereographic projections, where the rolled plate normal direction is at the centre, and the two rolling directions are at 3 O'clock and 12 O'clock.We will discuss these further in Lecture 7. In this case the measurement was made using electron backscatter diffraction (EBSD) in the SEM. Simultaneously, the composition at each point was measured using energy dispersive X-ray microscopy, which allowed the primary α and secondary α to be distinguished - because the primary α formed at a higher temperature, they contained more Al and less V. These are shown in the two colour plots.

What we observe is that there are three colonies in the primary α - coloured blue, purple and green, which have been coloured in the corresponding pole figure. For the secondary α, there are some additional orientations (denoted x in the (0002) pole figure), which correspond to

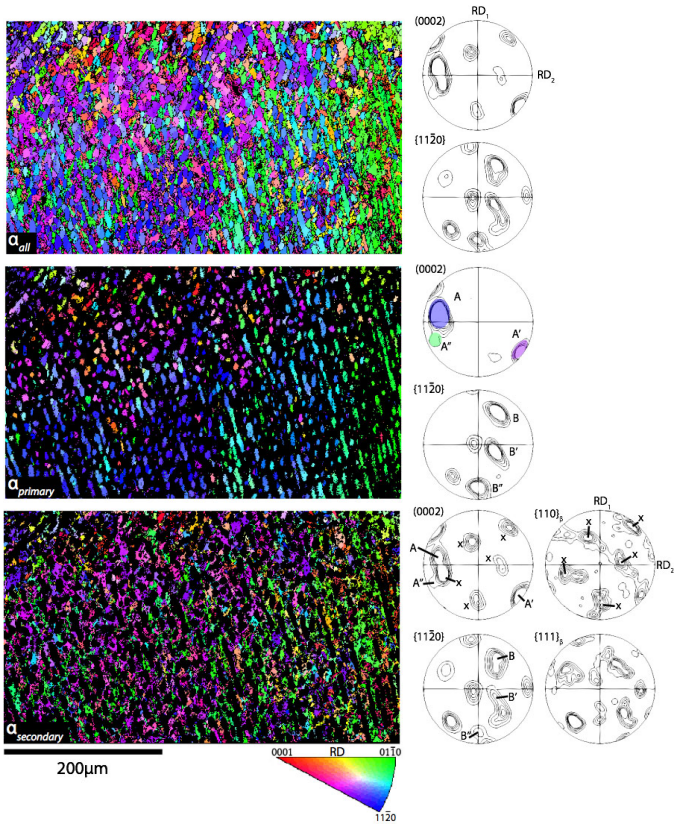

Figure 11: EBSD of the 4h rolled sample from Figure 9. The β in between the secondary α were not distinguishable at that time, so the secondary α also appear equiaxed in this plot. The α_p and α_s were partitioned based on composition. The colouration is shown in the inverse pole figure key diagram, with respect to the rolling direction of the plate. JL Warwick, Dye research group, 2013.

different variants of α that can form, but the majority of the secondary α is in the same orientation as the nucleating α_p.

6.2. Equiaxed microstructures

If the final globularisation is performed very low in the $\alpha+\beta$ field and/or the cooling rate from the globularisation is very slow, then instead of a bimodal microstructure, a fully equiaxed microstructure is produced, consisting only of primary α. In fact, the definition is slightly more subtle - that the primary α mostly touch each other. in this instance the equiaxed α have non-continuous β films at their grain boundaries. Two examples are shown in Figure 12.

Not that in any of these microstructures, because the α phase has limited solubility for the major β stabilisers (e.g. Mo and V), then the β may end up with a composition quite far from Ti - in the case of Ti-6Al-4V the $\sim 5\%$ β fraction is approximately of the composition Ti-20V.

6.3. Macrozones

Recently (since 2000) it has become clear that the regions of common orientation can extend over centimetres in the microstructure. In fact, this can be observed with

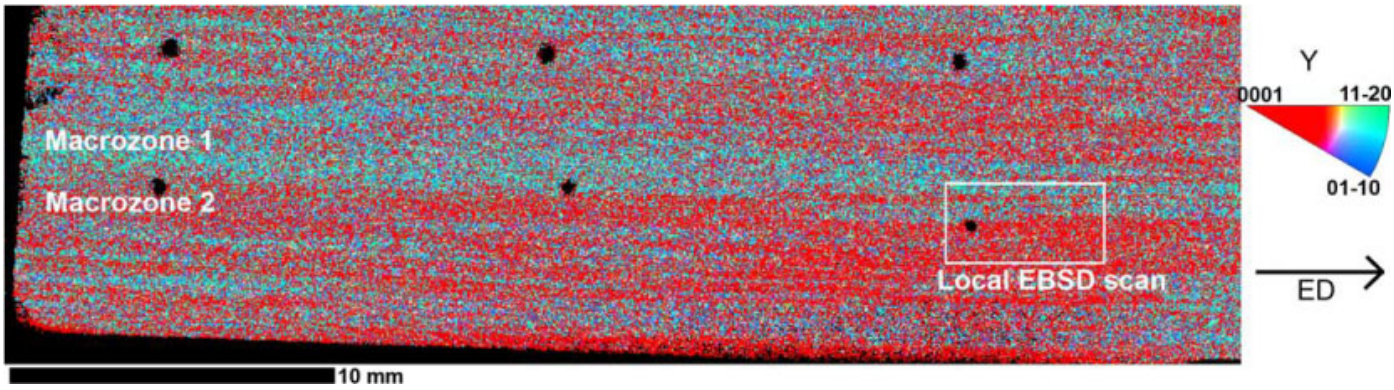

Figure 13: Presence of very large macrozones in IMI834 billet. From Germain et al, Acta Mater., 2005.

the naked eye in the right circumstances, just by observing as-rolled billets. But it took the development of EBSD to demonstrate it beyond doubt, as shown in Figures 13-14. There is significant concern, not yet fully substantiated, that these may have detrimental effects on fatigue performance. It is suggested that these arise from the original prior β grains that are pancaked during processing and which are never truly broken up and recrystallised.

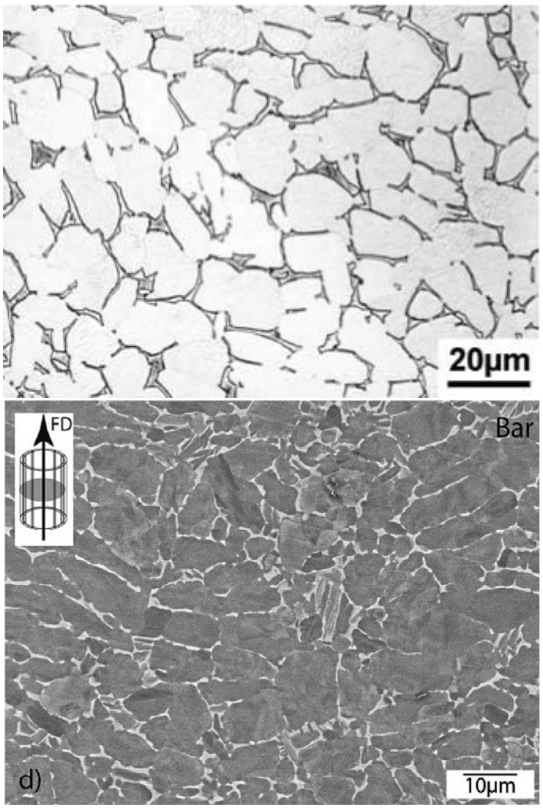

Figure 12: Equiaxed microstructures in Ti-6Al-4V. (top) from Lutjering and Williams, (bottom) I Bantounas, Dye research group, 2008.

6.4. Attempts to develop alternative microstructures

Heavily β stabilised alloys like Ti-5Al-5Mo-5V-3Cr (Ti-5553) are processed in similar ways to conventional alloys, but the primary α fraction is necessarily quite small. The approx. micron sized primary α do not provide much strengthening but serve merely to prevent β grain growth and allow the development of a β subgrain structure. Figure 15 shows the general scheme of processing. First, the material is slowly cooled from the β, allowing a colony microstructure to develop. The plates are then broken up by hot deformation just below the transus, into fine primary α. These are then aged, and secondary α developed, by a heat treatment in the $500 - 650°C$ range.

Ti-5553 is widely used, for instance in the truck beam forgings of the landing gear of the B787 and A350, and in the casing of some smaller jet engines. It has exceptional strength - around 1450 MPa in some heat treatment con-

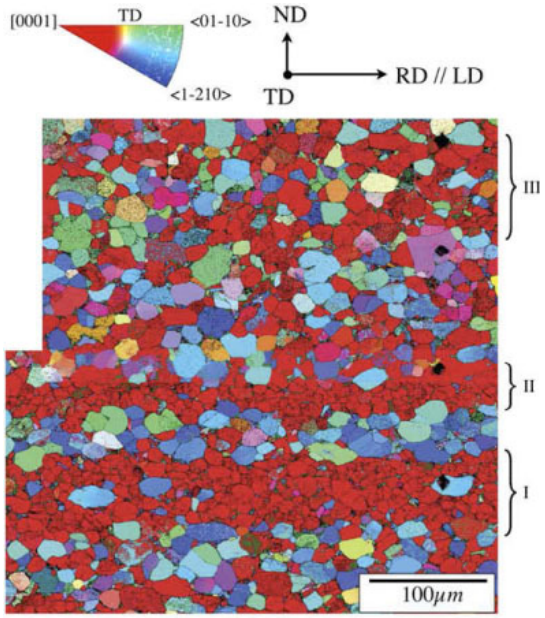

Figure 14: Macrozones in unidirectionally rolled, bimodal Ti-6Al-4V plate. The primary texture is with the (0002) ‖ TD. (bottom) I Bantounas, Dye research group, 2009.

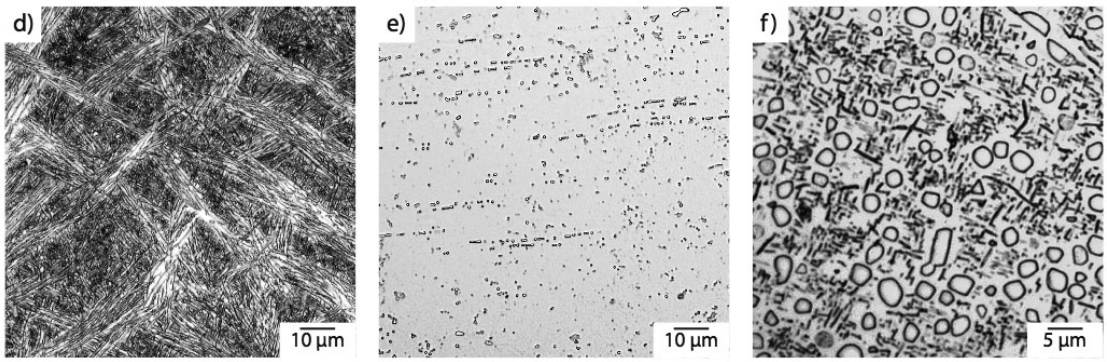

Figure 15: Conventional microstructures in Ti-5553; (d) transformed β microstructure, (e) $\alpha + \beta$ rolled from (d) and quenched, (f) heat treated to develop fine secondary α from (e). From Jones and Dye, 2011.

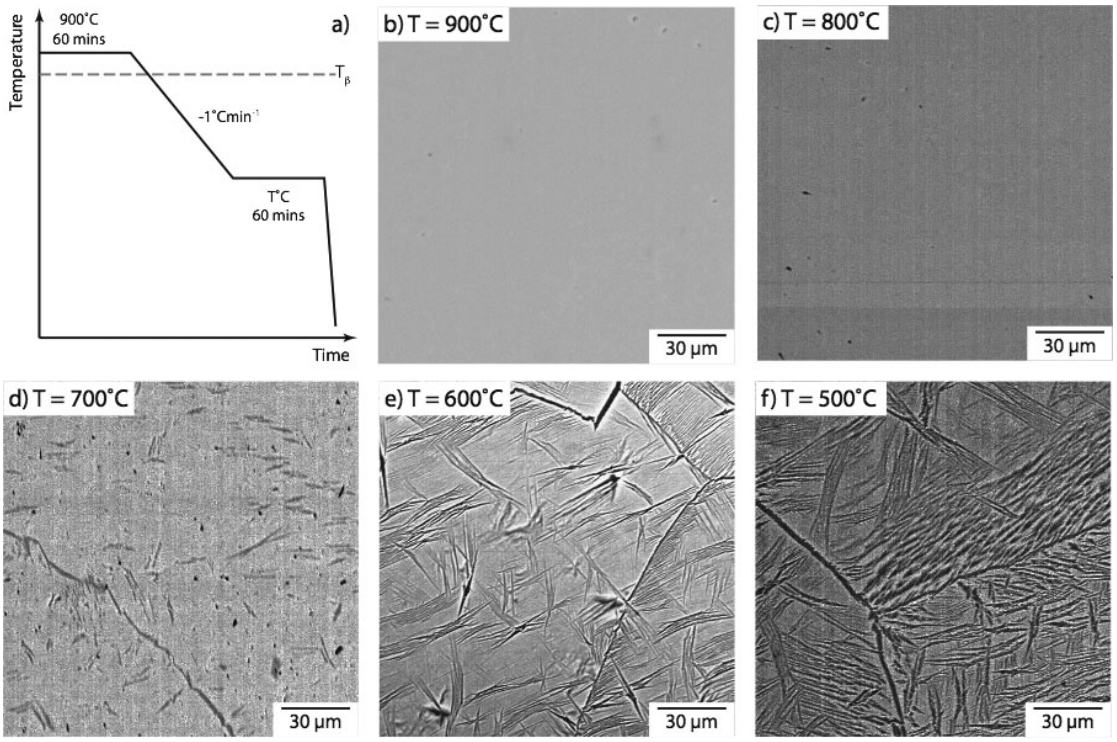

Figure 16: Ti-5553 subjected to the BASCA treatment with different hold temperatures. The final cooling was rapid; since the transus of Ti-5553 is $\sim 845°C$, (b) represents a quenched β structure. From Jones and Dye, 2011.

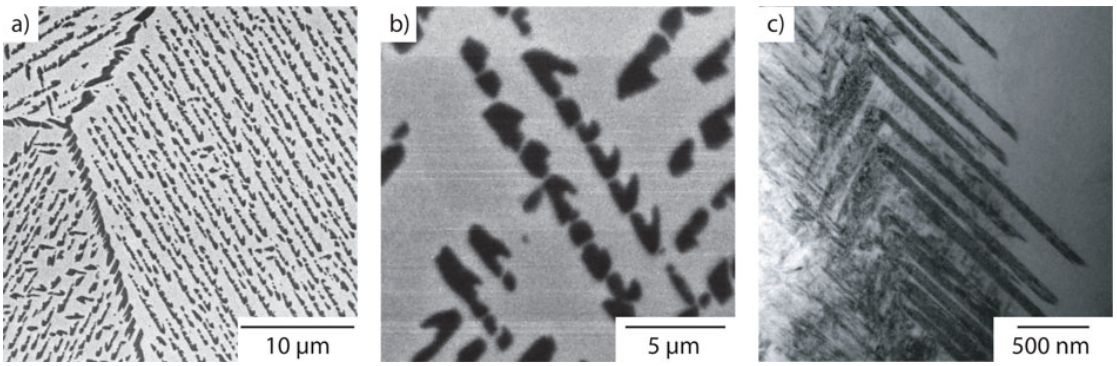

Figure 17: Ti-5553 β treatment followed by cooling to the ageing temperature of 400 °C for 8 h - termed 'direct ageing'. (a)-(b) BSEI, (c) TEM. From Jones and Dye, 2011.

ditions - and very high toughness. It also has very slow precipitation kinetics because of its high Mo content (slow diffusivity) and low transus (low temperature for transformation, low driving force), which also makes it an interesting subject of study for the development of novel Ti microstructures.

One example of these is the BASCA heat treatment recently patented (!) by Boeing. Here, the material is cold from the β very slowly, at $1\,\mathrm{K\,min^{-1}}$, to a hold temperature where it is held for 1 h, followed by quenching. One can observe, Figure 16, that until one gets to a hold temperature of 500°C, colony structures are generally not developed and that the grain boundary α remain relatively thin. However, interestingly, some intragranularly nucleated α does start to be visible in (e), which is very unusual for Ti alloys. For some of the 'starbursts' the nucleation site is even apparent.

Therefore it is apparent that in titanium, intergranular nucleation is *really* difficult. Another heat treatment variation in Ti-5553 is so-called direct ageing - cooling from the β directly to an ageing temperature, and holding, Figure 17. In this treatment, a radically different microstructure is obtained. The grain boundary α have become serrated - with so little diffusion, there can be less solute rejection. A precipitate free zone around the grain boundary α is also apparent, where β stabiliser has been rejected and therefore no α is present. But the dramatic observation is the chevron shaped α precipitates, formed into lines, that decorate the interior of the prior β grains. Closer examination of these chevrons shows that they are composed of a group of sympathetically nucleated α plates, around 50 nm thick and 1 µm long. The question is therefore how these formed to give such a different microstructure.

Returning to the isomorphous phase diagram, Figure 1, we observe that at high β stability another phase, ω, is noted. This is the high pressure phase of pure Ti, and is a hexagonal phase with a c/a ratio of 0.66 - 2/3 compared to a normal hcp c/a ratio of 3/2. It forms from the bcc phase by collapse of alternate {111}-type planes to form the B layers in the hexagonal ABAB packing structure. Examine Figures 18-19. Here we see that ω can form by

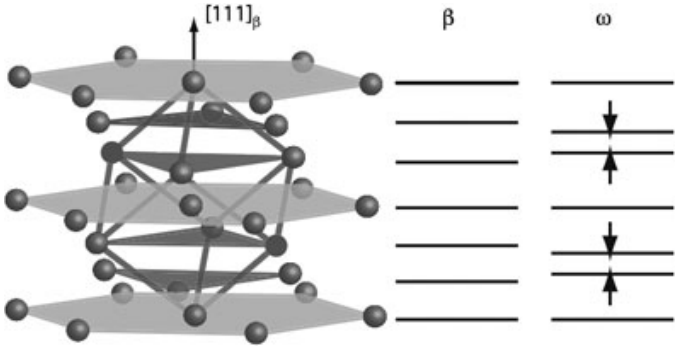

Figure 18: Schematic of the β unit cell's relationship to the ω structure. The intermediate {111} bcc planes collapse together to form the ω structure. From Talling, PhD thesis, Imperial College, 2008.

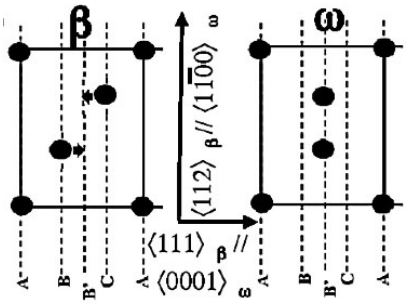

Figure 19: Schematic of the collapse process. bcc layers B and C, vibrating longitudinally, stick together to form the new ω layer B'.

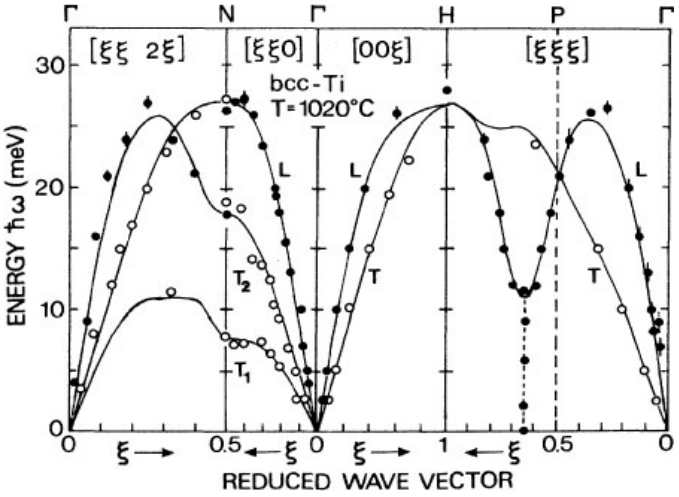

Figure 20: Phonon dispersion for bcc Ti at 1020°C. A soft mode is visible in the longitudinal curve (L) near [111]. From Petry et al, Phys Rev Lett, 1991.

only a very small rearrangement of some of the bcc planes. As it happens, in bcc Ti (and Zr and Hf) these planes have very large natural vibrations - a soft phonon mode - and so this transformation is relatively easy. This is shown in Figure 20.

Therefore it is observed that at very high undercoolings, bcc Ti can undergo transformation to the ω phase. ω formed on quenching is termed athermal ω and is typically very hard to observe directly in the TEM. Diffuse streaks are often observable in the $g = [110]$ and $g = [113]$ zone axis diffraction patterns, though. Banerjee has recently suggested that the transformation sequence is first a spinodal decomposition of the β, as indicated by the Ti-Mo phase diagram (see Lecture 5 notes). Then, the relatively pure β can transform to ω if it is to the left of the T_0 point, Figure 21.

In the right circumstances, ω can be imaged directly, such as in Figure 22. The classic ω ageing temperature is 300 °C, and of course an 1150 hour heat treatment is meant only to prove the point - that the diffuse streaks observed in TEM can eventually be aged to the point where precipitates can be imaged.

All of this discussion of ω is intended to persuade you

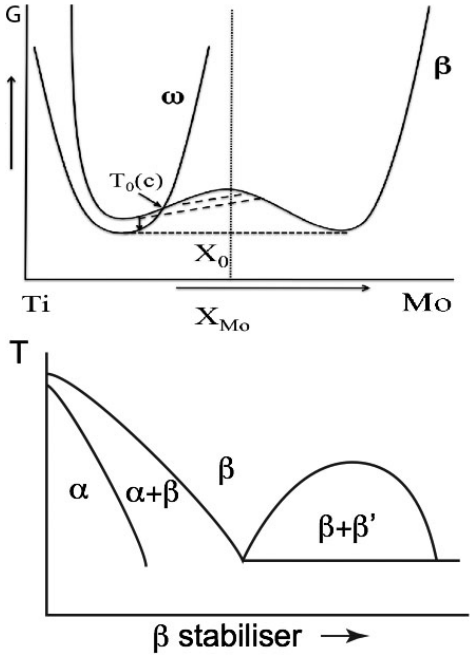

Figure 21: (top) Hypothetical Gibbs Energy curve for ω formation, From Banerjee et al, Phys Rev Lett, 2012. Bottom, implied equilibrium phase diagram.

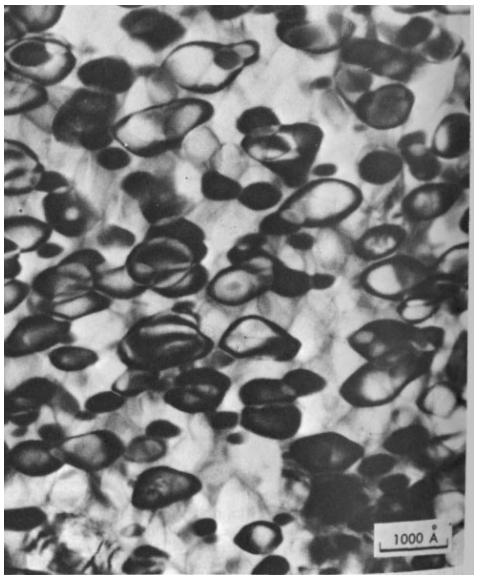

Figure 22: Observation of ω phase precipitates in Ti-11.6Mo-0.1O (wt%) after 1150 hr ageing at 400°C, DF TEM. From Blackburn and Williams, Trans of the AIME, 1968.

that the β we observe to be retained on quenching often isn't really very stable. For this reason, 3 wt.% Al is added to most metastable β alloys in order to suppress ω formation, as ω is generally found to be embrittling.

But, it does appears to be possible to use ω to precipitate intragranular α phase. Figure 23(a) shows X-ray diffraction patterns gathered using synchrotron X-ray diffraction, with sub-s time resolution. This allows the evolution of the diffraction pattern to be tracked through

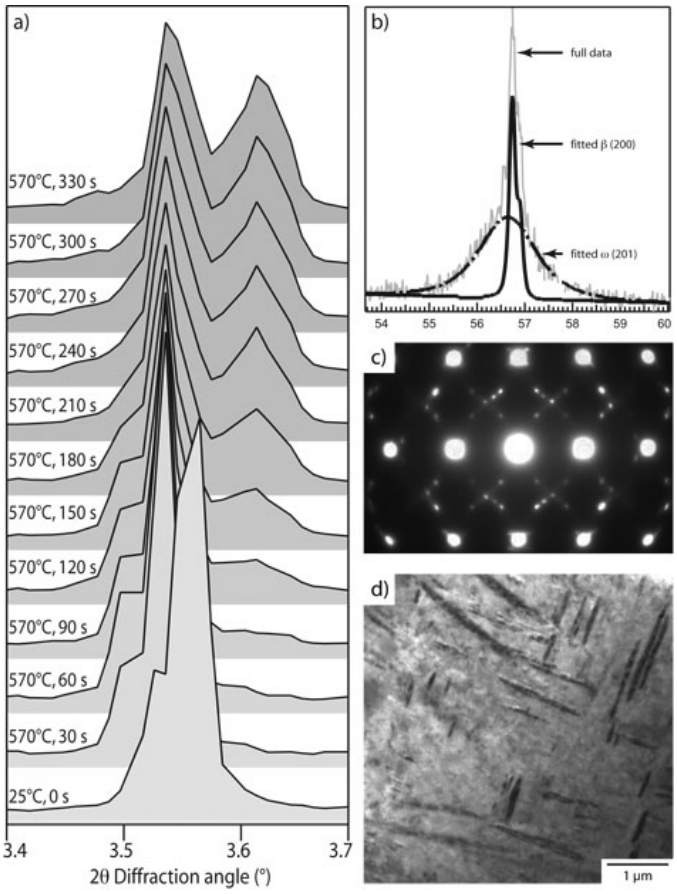

Figure 23: (a) Evolution of the β {200} diffraction peak on quenching Ti-5553, then reheating to 570°C. On quenching, a shoulder due to athermal ω appears, which disappears on reheating as the α phase gradually precipitates over the first few minutes. (b) fitted lab. X-ray diffraction peak on queching; (c-d) selected area diffraction pattern and bright field TEM image of the microstructure after 30 min at 570°C.

a very rapid quench from the β to room temperature, followed by flashing reheating to an α ageing temperature of 570°C.

What is observed is that on quenching a shoulder due to the ω appears. On reheating, it then disappears, but only as the α precipitates - the omega isn't a martensite that disappears on reheating, but it is the nucleation source for the α that precipitates.

This suggests that ω may have been the nucleation site for the intergranular α seen in Figure 17, although this is slightly speculative - but the temperature is correct for a $\beta \rightarrow \omega \rightarrow \alpha$ precipitation sequence.

As a final note, Figure 24, several authors (N Clement in Louvain and JC Williams in 1968) have found that α can also be precipitated on dislocations, intergranularly in the β.

6.5. Summary

In summary, the $\beta \rightarrow \alpha$ phase transformation and its crystallography dominates Ti metallurgy. As in steels, it is

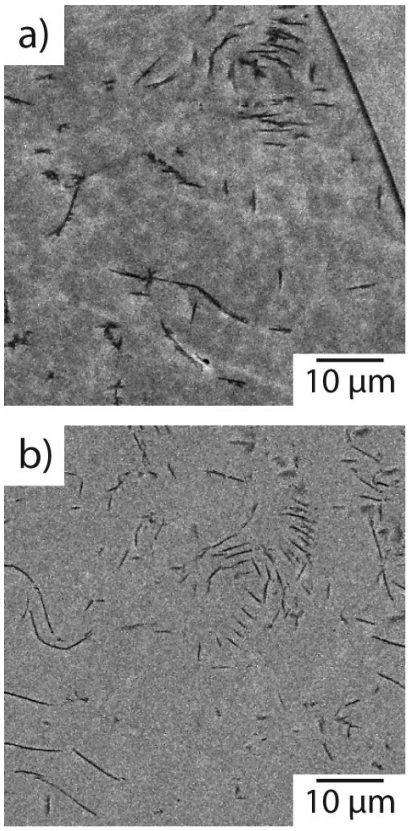

Figure 24: Ti-5553 quenched from the β and then flash aged at (a) 700°C and (b) 800°C for 5 min. Curved α precipitates are observed within the grain using BSEI, suggesting heterogenous nucleation from, e.g. dislocations.

very hard to prevent colony formation from grain boundary α (but it is possible in some heavily β stabilised alloys). The recrystallisation of hot worked α laths is the main route used to achieve a fine grain size, but macrozones inherited from the prior β grains are still found. In heavily β stabilised alloys, there are other possibilities associated with the decomposition of retained β.

— END OF LECTURE —